Journal of the Korean Nuclear Society
Volume 35, Number 4, pp.299~308, August, 2003

$(Th,U)O_2$ Pellets : Fabrication and Thermal Properties

Ki Won Kang, Jae Ho Yang, Keon Sik Kim, Kun Woo Song, Chan Bock Lee, and Youn Ho Jung
Korea Atomic Energy Research Institute
150 Dukjin-dong Yuseung-gu, Daejeon 305-353, Korea
kwkang@kaeri.re.kr

(Received December 3, 2002)

Abstract

Fabrication technique of $(Th,U)O_2$ pellets has been investigated. Powder mixtures of ThO_2 and UO_2 were milled in two different ways - dry and wet milling. Milled powder was compacted and sintered to $(Th,U)O_2$ pellets. The wet-milled powder leads to a $(Th,U)O_2$ pellet having a high sintered density and uniform distribution of U and Th, compared to the dry-milled powder. The sintered density of a $(Th,U)O_2$ pellet tends to decrease by increasing the content of ThO_2. The thermal conductivity of ThO_2 and $(Th,U)O_2$ pellets was measured by the laser flash method. The thermal conductivity of the ThO_2 pellet is higher than that of the UO_2 pellet, and the thermal conductivities of $(Th,U)O_2$ pellets containing 65wt% and 35wt% ThO_2 pellets are lower than that of the UO_2 pellet.

Key Words : $(Th,U)O_2$ pellets, wet and dry-milled powder, thermal conductivity, sintered density

1. Introduction

Thorium oxide (ThO_2) has recently attracted much attention as a nuclear fuel since it is resistant to proliferation and the amount of uranium oxide is limited [1]. Thorium is not fissile but can be converted into U-233 which is a fissionable isotope.

ThO_2 pellets can be fabricated, like UO_2 pellets, through ceramic powder processing; powder preparation, mixing, pressing and sintering. It is generally agreed that powder properties such as surface area and particle size influence greatly the methods of mixing and sintering. The surface area of UO_2 powder ranges from 2 to 5 m^2/g, and the green pellet of UO_2 powder can be sintered at about 1700℃. It should be noted that the melting point of ThO_2 is 3300℃ and is higher by 500℃ than that of the UO_2. This implies that the sintering of ThO_2 requires a higher temperature than that of UO_2. However, it is very difficult and uneconomical to raise the sintering temperature of

ThO_2 above 1800℃. So it is very important in ThO_2 pellet fabrication to prepare ThO_2 powder which can be sintered at comparatively low temperatures.

The sintering activity of ThO_2 powder generally increases by increasing the surface area of the powder, and the surface area is dependent on the preparation methods. Thorium oxide powder is commonly prepared by the calcining thorium oxalate[2] or sol-gel method [3,4]. Thorium oxalate is precipitated by adding oxalic acid to a thorium nitrate solution, and then ThO_2 powder is produced by the calcination of thorium oxalate. The sol-gel method consists of the preparation of a sol, conversion of the sol into a dried gel and calcination of the gel into high density microspheres. The surface area of ThO_2 powder is between 1 and 50 m^2/g[2]. Theses values are much larger than the surface area of UO_2 powder.

Mixed oxide pellets -$(Th,U)O_2$ pellets- can be fabricated by sintering the mixture of ThO_2 and UO_2 powders. Other mixed oxide pellets -$(U,Pu)O_2$ and $(U,Gd)O_2$ pellets- have also been fabricated in a similar way. Mixed oxide pellets are generally more difficult to fabricate than single oxide pellets since it is difficult to get a homogeneous mixture of two different powders by mechanical mixing or milling. Moreover, the sintering of two powders should include not only densification but also the formation of a solid solution. For example, the densification of mixed UO_2 and Gd_2O_3 powders is retarded by the formation of a $(U,Gd)O_2$ solid solution when $(U,Gd)O_2$ pellets are sintered [5].

Thermal conductivity is one of the most important properties of nuclear fuel. It is well known that the thermal conductivity of ThO_2 is high compared to that of UO_2[4]. However, the thermal conductivity of $(Th,U)O_2$ is relatively unknown.

This work investigates the fabrication methods of ThO_2 and $(Th,U)O_2$ pellets and especially, deals with powder milling methods for getting high pellet density and uniform distribution of U and Th. This paper also describes the thermal conductivity of ThO_2 and $(Th,U)O_2$ pellets.

2. Experimental Procedures

Thorium oxide (ThO_2) powder(>99.9%) was purchased from Indian Rare Earth LTD. According to the supplier' s information, this powder was produced by calcining thorium oxalate. The as-received powder was characterized by the BET surface area measurement, particle size, X-ray diffraction and SEM. X-ray diffraction was performed using Cu Kα radiation with a monochromator. Pellets of ThO_2, UO_2-65wt%ThO_2, and UO_2-35wt%ThO_2 were fabricated using three different powders; as-received, dry-milled and wet-milled powders.

2.1. Dry Milling

The as-received ThO_2 powder was milled in a mortar for 40 min. For ThO_2 pellet fabrication, this powder was milled further by passing it 6 times through the attrition mill which consisted of zirconia balls, an impeller and a jar with an inlet and an outlet for powder charge. Especially, the outlet on the bottom of a jar is a grid-shaped hole, so the milled powder can pass continuously through the hole and is stored in a bottle. The powder in a bottle is then put again into a feeding hopper attached to the attrition mill. Powder was milled 6 times in this way. Powder charge was milled by zirconia balls driven by an impeller rotating at a speed of 150 rpm.

For $(Th,U)O_2$ pellet fabrication, the ThO_2 powder, which was previously milled in a mortar for 40 min, was mixed with UO_2 powder ex-ADU in a tumbling mixer for 1h. ThO_2 contents of the powder mixtures are 35 and 65wt%. Each

powder mixture was milled 6 times through an attrition mill in the same method as the above-mentioned.

2.2. Wet Milling

The as-received ThO_2 powder was mixed with the UO_2 powder ex-ADU in a tumbling mixer for 1h to form powder mixtures. ThO_2 contents of the powder mixtures are 35 and 65wt%. The powder mixtures were ball-milled for 24h in a jar containing zirconia balls and alcohol and then dried in air for more than 3 days at ambient temperatures. The as-received ThO_2 powder was also ball-milled in the same way.

2.3. Compaction, Sintering and Thermal Etching

The prepared powders were pressed at 2, 3 and 4 ton/cm^2 into compacts (green pellets). The compacts were heated up to 1700℃ with a heating rate of 5℃/min and then held for 4 h in a H_2 atmosphere to fabricate the sintered pellets. The density of the sintered pellets was determined by the water immersion method. The theoretical density of the (Th,U)O_2 pellets was determined by considering each theoretical density of ThO_2 and UO_2 in accordance with each mole fraction. Theoretical density of pure ThO_2 is 10.00g/cm^3 and the calculated theoretical density of 65wt%ThO_2, 35wt%ThO_2 are 10.33g/cm^3 and 10.62 g/cm^3, respectively.

Sintered pellets were sectioned longitudinally and polished. In order to observe grain boundaries thermal etching was carried out at 1600℃ for 4h in a H_2 atmosphere, and the grain size was determined by the linear intercept method.

X-ray diffractometry on (Th,U)O_2 pellets was carried out to ascertain if the ThO_2-UO_2 solid solution had been formed. EPMA(Electron Probe Micro Analysis) was performed on the polished pellet surface to examine the distribution of U and Th.

3. Results and Discussion

3.1. Characteristics of As-received ThO_2 Powders

Fig. 1 shows the SEM micrograph of the as-received ThO_2 powder. The photograph shows that the particle is rough or porous. The BET surface area of this powder is 41.16m^2/g, and the average size is 10㎛. According to the available literature[2], the BET surface area of ThO_2 powder is quite dependent on the calcination temperature and ranges from 1 to 50 m^2/g.

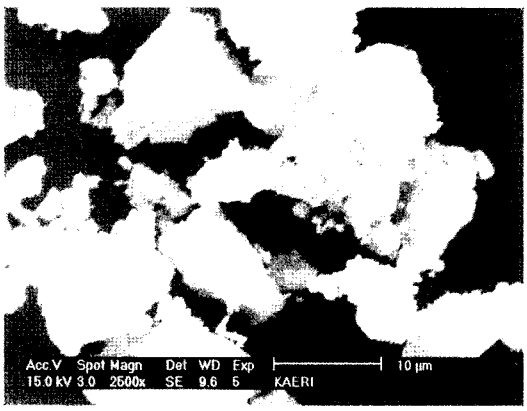

Fig. 1. SEM Photograph of as-received ThO_2 Powder

3.2. Properties of Pellets Fabricated from the Dry-Milled Powders

Fig. 2 shows the green density of the as-received ThO_2, milled ThO_2 and milled UO_2-ThO_2 powders for different compacting pressures. The green density of all the powders increases with the compacting pressure. When the as-received ThO_2

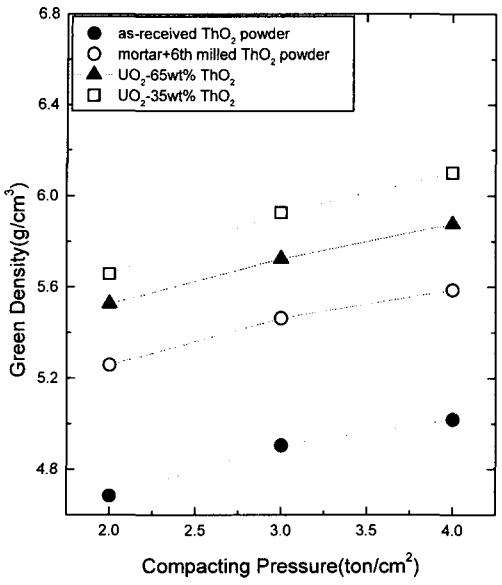

Fig. 2. Green Density as a Function of Compacting Pressure for Dry-milled Powder

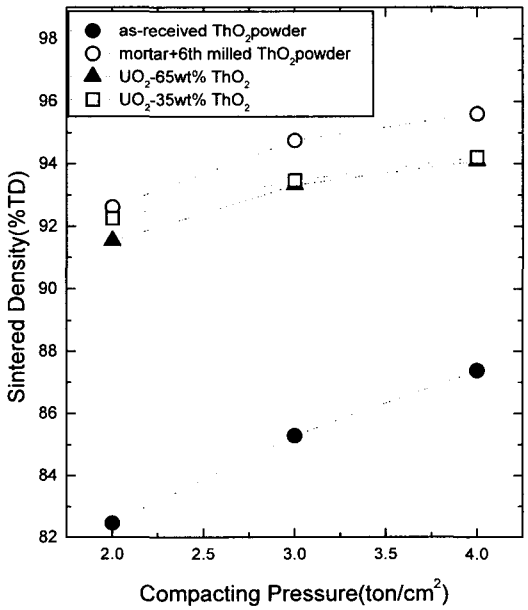

Fig. 3. Sintered Density as a Function of Compacting Pressure for Dry-milled Powder

is compared with the dry-milled ThO_2, it is found that the green density is greatly increased by dry milling. The dry milling might break the porous structure of the as-received ThO_2 powder and thus can improve the green density.

Fig. 3 shows the sintered density of the as-received ThO_2, milled ThO_2 and milled UO_2-ThO_2 pellets for different compacting pressures. All the powders tend to get higher densities as the compacting pressure increases. For the as-received ThO_2 powder the sintered density of 85~88%TD is obtained, depending on the compacting pressure applied. It is known [6] that the sintered density of pure ThO_2 powder depends greatly on the calcination temperature. The above range of sintered densities agrees well with other reported values [2]. The sintered density of milled ThO_2 pellets range from 92 to 95%TD, depending on the compacting pressure. This density is higher by about 7%TD than that of the as-received powder. This means that the combined mortar and attrition milling is effective in increasing the sintering activity of the ThO_2 powder. The sintered density of $(Th,U)O_2$ pellets range from 91% to 94%TD, which is slightly lower than that of the milled ThO_2 pellets. This slight difference in sintered density between the two pellets might result from the differences in composition and green density.

Fig. 4(a) shows the XRD patterns of pure UO_2, ThO_2 and $(Th,U)O_2$ pellets, and fig. 4(b) shows the same results at high 2θ angles. Fig. 4(b) shows that ThO_2 has a larger lattice constant than UO_2, and that the peaks shift towards the high angles as the content of UO_2 increases. The UO_2-65wt%ThO_2 and UO_2-35wt%ThO_2 pellets show single peaks similar to the UO_2 or ThO_2 pellet, indicating that solid solutions were formed to some extent. But it is supposed that the solid solution is not yet fully formed since the FWHM (Full Width Half Maximum) of the peaks is wider than that of pure

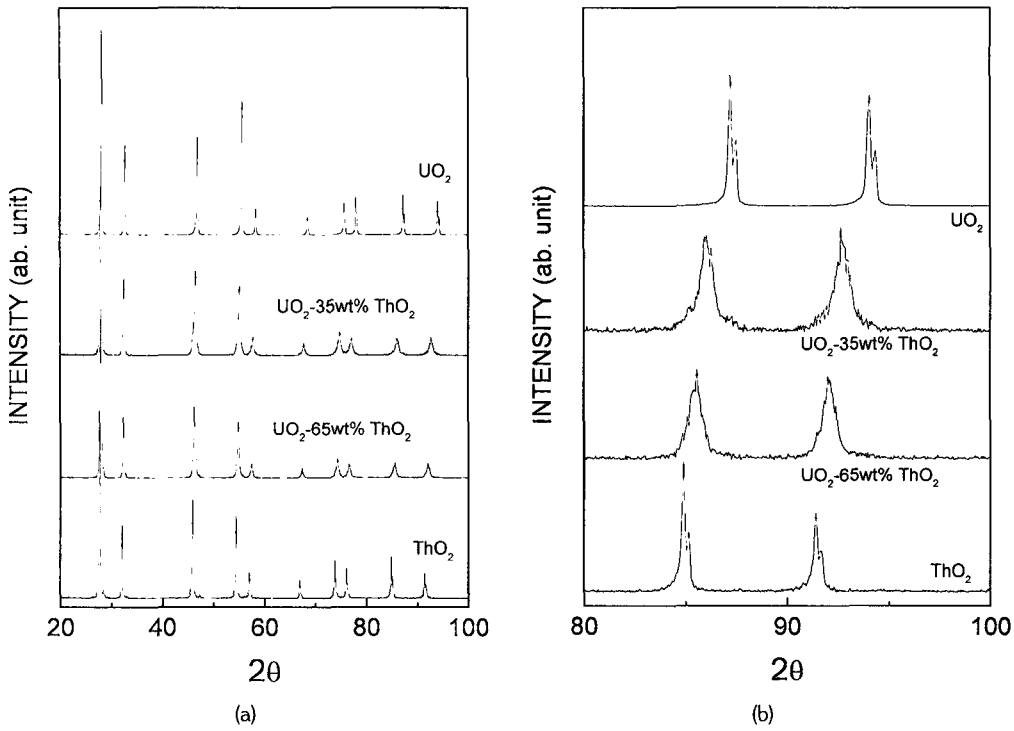

Fig. 4. X-ray Diffraction Patterns for Pure UO_2, ThO_2 and (Th,U)O_2 Pellets with Dry Milled Powder

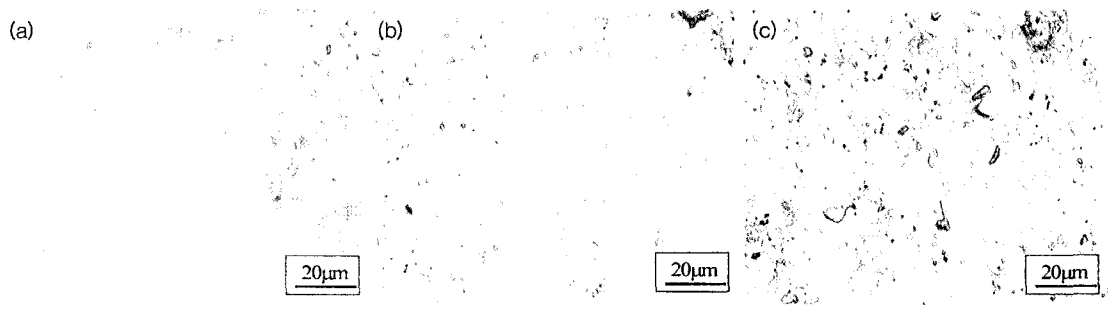

Fig. 5. Microstructure of Pellets Fabricated from Dry-milled Powder (a) Pure ThO_2, (b) UO_2-65wt%ThO_2, (c) UO_2-35wt%ThO_2

UO_2 or ThO_2.

Fig. 5(a), 5(b) and 5(c) show the respective microstructures of ThO_2, UO_2-65wt%ThO_2 and UO_2-35wt%ThO_2 pellets whose green pellets were pressed at a compacting pressure of 4 ton/cm^2. Some round areas that were different in color from the surrounding matrix were observed in Figs. 5(b) and 5(c), suggesting that a solid solution might not be completely formed. The above-mentioned X-ray diffraction pattern also indicated that the solid solution of (Th,U)O_2 was incompletely formed. The grain sizes were 8.6㎛ for ThO_2, 5.5㎛ for UO_2-65wt%ThO_2 and 5.3㎛ for UO_2-35wt%ThO_2 pellets, indicating that the

grain size of a $(Th,U)O_2$ pellet is smaller than that of a ThO_2 pellet.

3.3. Properties of Pellets Fabricated from the Wet-Milled Powders

Fig. 6 shows the green density of the wet-milled ThO_2 and UO_2-ThO_2 powders for different compacting pressures. The green density of wet-milled powders increases with the compacting pressure. When the wet-milled ThO_2 is compared with the as-received ThO_2, it is found that the wet-milling increases the green density of the powder. Fig. 7 shows the sintered density of the wet-milled ThO_2 and UO_2-ThO_2 pellets for different compacting pressures. All the pellets have a higher density than 95%TD, but the highest sintered density of the pellets for every composition is achieved at the compacting pressure of 3 ton/cm^2. However, the sintered density increases with the compacting pressure when the dry-milled powder is used. The relation between the sintered density and the compacting pressure might be influenced by the difference in the powder milling method.

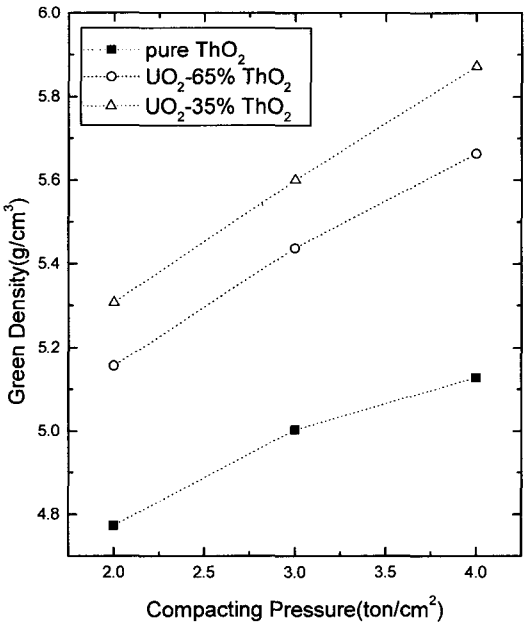

Fig. 6. Green Density as a Function of Compacting Pressure for Wet Milled Powder

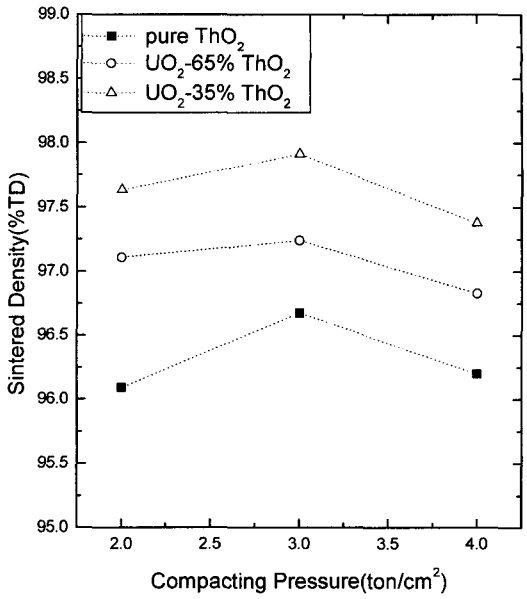

Fig. 7. Sintered Density as a Function of Compacting Pressure for Wet-milled Powder

Fig. 8(a) shows the XRD patterns for ThO_2 and $(Th,U)O_2$ pellets, and Fig. 8(b) shows the same results at high 2θ angles. The peak position and its relative intensity are the same as those for the dry-milled pellets(see fig. 4). But the FWHM of the peaks is sharper in the wet milled pellets than in the dry milled pellets, so it is supposed that the $(Th,U)O_2$ solid solution is more homogeneous for the wet-milled powder than for the dry-milled powder.

Fig. 9 shows the lattice parameters of $(Th,U)O_2$ pellets determined by X-ray diffraction. The lattice parameters of wet-milled pellets follow Vegard' s law very closely, but those of dry-milled pellets depart from Vegard' s law. This means that a solid

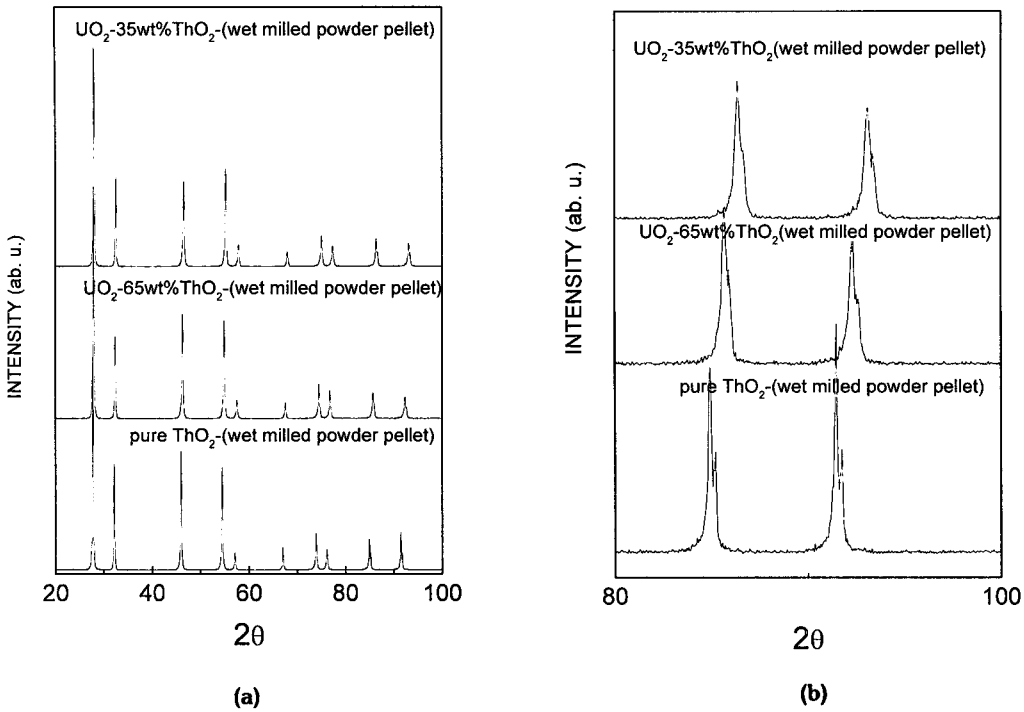

Fig. 8. X-ray Diffraction Patterns of ThO_2 and (Th,U)O_2 Pellets for Wet-milled Powder

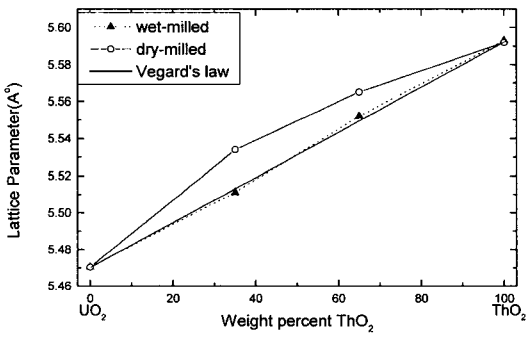

Fig. 9. Lattice Parameter of the UO_2-ThO_2 Pellets

solution is more completely formed in wet milled pellets than in dry milled pellets since the lattice parameter of an ideal solid solution follows Vegard' s law[7]. The lattice parameters of UO_2-ThO_2 found in this work were 5.534 Å(dry-milled) and 5.511 Å(wet-milled) for UO_2-65wt%ThO_2 and 5.565 Å(dry-milled) and 5.552 Å(wet-milled) for UO_2-35wt%ThO_2.

Fig. 10(a), 10(b) and 10(c) show the respective microstructures of pure ThO_2, UO_2-65wt%ThO_2 and UO_2-35wt%ThO_2 pellets whose green pellets were pressed at a compacting pressure of 3 ton/cm^2. The color difference found in the dry-milled pellet is not observed in the wet-milled pellet. The grain size were 11.2㎛ for ThO_2, 9.2 ㎛ for UO_2-65wt%ThO_2 and 7.5㎛ for UO_2-35wt%ThO_2 pellets. The grain sizes of wet-milled pellets are larger than those of dry-milled pellets. This result might be related with the fact that the solid solution is more complete in the wet-milled pellet than in the dry-milled pellet.

Fig. 11(a) and (b) show the results of area mapping(uranium scanning) of the UO_2-65wt%ThO_2 and UO_2-35wt%ThO_2 pellets, respectively. Local regions are not found which

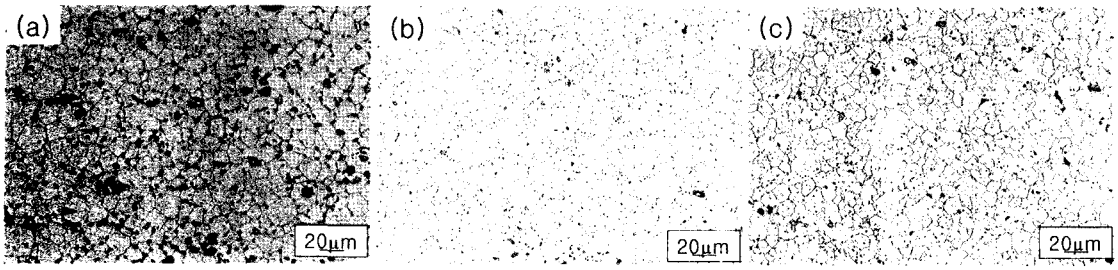

Fig. 10. Microstructure of Pellets Prepared from Wet-milled Powder (a) Pure ThO_2, (b) UO_2-65wt%ThO_2, (c) UO_2-35wt%ThO_2

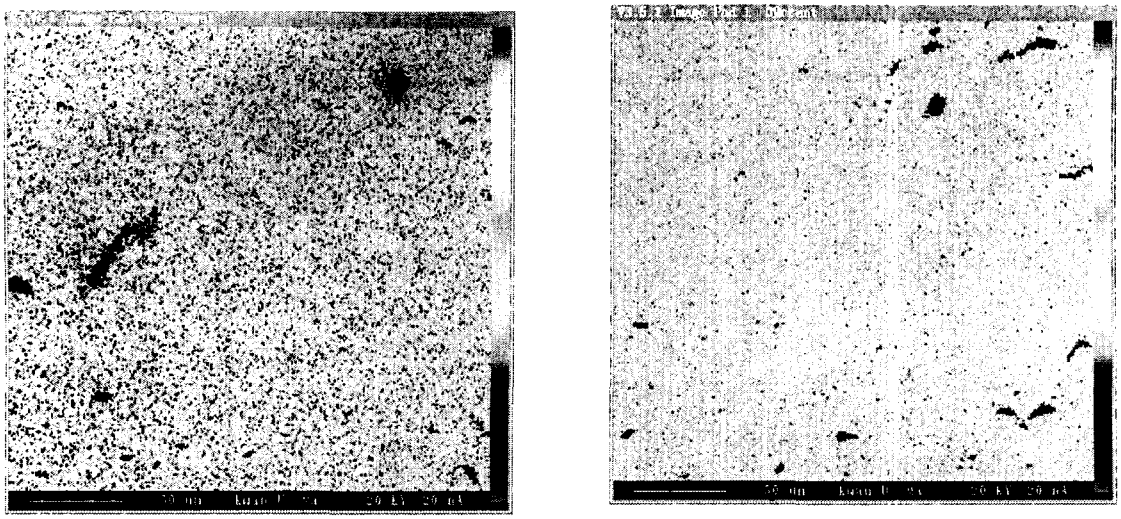

(a) UO_2-65wt%ThO_2 **(b) UO_2-35wt%ThO_2**

Fig. 11. EPMA of the UO_2-65wt%ThO_2 and UO_2-35wt%ThO_2 Pellets (uranium scanning)

are rich or poor in U concentration, so the wet-milled pellet is uniform in U and Th distribution.

3.4. Thermal Conductivity of (Th,U)O_2 Pellet

The pellets for measuring the thermal properties were fabricated using the wet milled powder. From the measured thermal diffusivity, the thermal conductivity was calculated using the following relation

$$\kappa = \alpha C_p \rho$$

where κ, α, ρ, C_p are the thermal conductivity, thermal diffusivity, the bulk density and the specific heat capacity of the sample, respectively. The thermal diffusivity of the pellets was measured by the laser-flash method (Laser-flash 2000, Sinku Rico). Heat capacity was measured using a differential scanning calorimeter (DSC).

Fig. 12 shows the schematic diagram of the thermal diffusivity measurement apparatus. The thermal diffusivity was determined from the rear-surface temperature rise to reach its half maximum value, after the front surface of the sample was

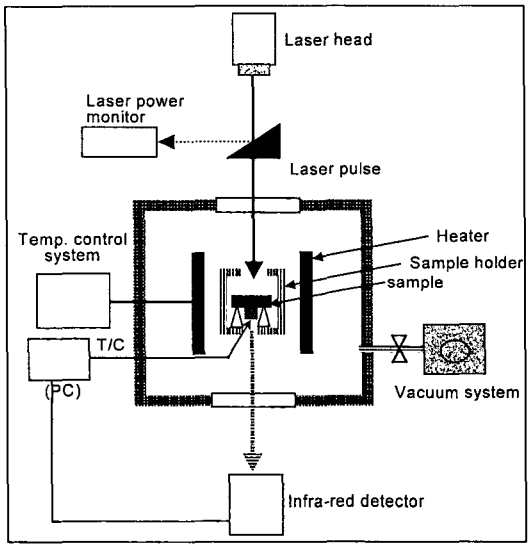

Fig. 12. Schematic Diagram of the Thermal Diffusivity Measurement Apparatus

heated by the laser beam.

$$\alpha = \frac{\omega}{\pi^2}\frac{L^2}{t_{1/2}}$$

where, L is the sample thickness.

The obtained thermal conductivity was normalized to 95% of the theoretical density using the modified Loeb equation[8].

$$\kappa = \kappa_{TD}\left(1-\beta\left(1-\frac{\rho}{\rho_{TD}}\right)\right)$$

where, β is constant.

Fig. 13 shows the thermal conductivity of ThO_2 together with the other data [9]. This data is corrected with regards to 95% theoretical density. Our result is in resonable agreement with other results. Fig. 14 shows the results of thermal conductivity for ThO_2 and (Th,U)O_2 pellets. For comparison, the thermal conductivity data of UO_2 is taken from Fink' s work[10]. The thermal conductivity of (Th,U)O_2 decreases with UO_2 content over the whole temperature range. It is found that the thermal conductivity of (Th,U)O_2

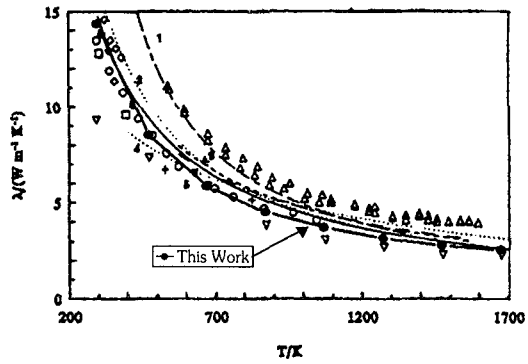

Fig. 13. The Thermal Conductivity of ThO_2 [8]

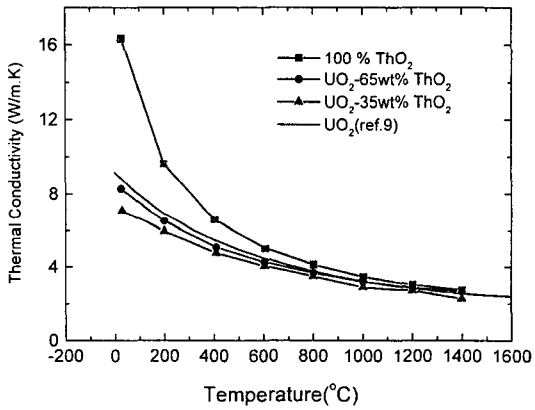

Fig. 14. Plot of Thermal Conductivity as a Function of Temperature

containing 35wt% and 65wt% ThO_2 is slightly lower than that of either ThO_2 or UO_2. When two materials form a complete solid solution, it is common and correct that the thermal conductivity of that solid solution is lower than the average value predicted by the mole fraction. Therefore, the measurement result of thermal conductivity for (Th,U)O_2 pellets may be resonable values.

4. Conclusions

1. The fabrication method of wet-milling ThO_2-UO_2 powder and sintering at 1700℃ produces (Th,U)O_2 pellets having a density of 94 to 98%TD.

2. Wet-milling of ThO_2-UO_2 powder is more effective in improving the pellet properties such as sintered density, grain size and homogeneity than dry-milling.
3. The thermal conductivity of ThO_2 is higher than that of UO_2, and the thermal conductivities of $(Th,U)O_2$ pellets containing 35wt% and 65wt% ThO_2 are slightly lower than that of UO_2.

Acknowledgements

This work has been carried out under the Nuclear R&D Program supported by MOST, Korea.

References

1. M. Kanno, S. Kokubo and H. Furuyal., "Preparation of thorium-uranium mixed oxide pellets", Journal of Nuclear Science and Technology, 19(11), 956-958(1982).
2. J. M. Pope and K. C. Radford, "Physical properties of some thoria powders and their influence on sinterability", Journal of Nuclear Materials, 52, 241-254(1974).
3. S. Anthonysamy, K. Ananthasivan, V. Chandramouli, I. Kaliappan, and P.R. Vasudeva Rao, "Combustion synthesis of urania-thoria solid solutions", Journal of Nuclear Materials, 278, 346-357(2000).
4. P. Rodriguez and C. V. Sundaram, "Nuclear and materials aspects of the thorium fuel cycle", Journal of Nuclear Materials, 100, 227-249(1981).
5. K. W. Kang, S. K. Kim, K. W. Song, J. H. Yang and Y. H. Jung, "Effect of TiO_2 and $Al(OH)_3$ on sintering behavior of UO_2-Gd_2O_3 fuel pellets", Journal of the Korean Nuclear Society, 32, 559-565(2000)
6. Y. Harada, Y. Baskin and J. H. Handwerk, "Calcination and sintering study of thoria", J of American Ceramic Society, 45, 253-257(1962)
7. I. Cohen and R. M. Berman, "A metallographic and X-ray study of the limits of oxygen solubility in the UO_2-ThO_2 system", Journal of Nuclear Materials, 18, 77-107(1966).
8. A.L. Loeb, J. Am. Ceram. Soc. 37, 96(1954).
9. K. Bakker, E. H. P. Cordfunke, R. J. M. Konings, R. P. C. Schram,"Critical evaluation of the thermal properties of ThO_2 and $Th_{1-y}U_yO_2$ and a survey of the literature data on $Th_{1-y}Pu_yO_2$", J. Nuclear Materials, 250, 1-12(1997)
10. J. K. Fink, Journal of Nuclear Materials, 279, 1-18(2000).